

## Letter to the Editor

# Design and testing of a simple structural component for space applications

Juraj Koráb\*, Stanislav Kúdela, Jr., Pavol Štefánik, František Simančík, Naďa Beronská, Peter Tobolka<sup>†</sup>

*Institute of Materials and Machine Mechanics, Slovak Academy of Sciences,  
Dúbravská cesta 9, 845 13 Bratislava, Slovak Republic*

Received 24 January 2022, received in revised form 2 May 2022, accepted 2 May 2022

### Abstract

The paper presents the designing, technology, and characterising mechanical and damping properties of two types of structural components that might be useful in space applications. The components (struts) were produced by the gas pressure infiltration of molten Mg into a preform of continuous carbon fibres. For comparison, also a non-reinforced component from pure Mg was prepared. Vibroacoustic tests showed that the samples reinforced with carbon fibres had better damping – approximately two times higher loss factor ( $\eta = 0.0018$  and  $\eta = 0.0021$ ) than the cast Mg component ( $\eta = 0.0008$ ). The bending tests confirmed the results obtained by vibroacoustic testing and revealed that the stiffness of the reinforced structural component was approximately six times higher than that of the unreinforced Mg material.

**Key words:** metal matrix composites, magnesium matrix, carbon fibre, gas pressure infiltration, space application

### 1. Introduction

The main prerequisite for all structural components launched onto orbit is the minimum weight, which makes it possible to reduce the cost of overcoming gravity to the lowest possible level. The load-bearing structures and fastening elements must be strong and stiff and have low thermal expansion. To stabilise space structures, good damping in a wide frequency range is also needed to suppress mechanical vibrations. In space applications, the modulus of elasticity ( $E$ ) of used materials needs to be maximised for a given density ( $\rho$ ), whereas suitable lightweight structural materials need to possess the highest  $E/\rho$  ratio. The  $E/\rho$  ratio of traditional metals is practically the same and far below that of optimized composites [1, 2].

As not all requirements can be met with conventional materials, metal matrix composites (MMCs), which provide good mechanical and thermophysical properties at elevated temperatures, are used [3–5].

Therefore, the future structural material should consist of a lightweight, strong, and stiff reinforcement in combination with a very light metal matrix. If the stiffness of composite materials is to be comparable with steel, carbon fibres with a modulus of elasticity higher than 500 GPa can be used. The fibres have low density and excellent mechanical and thermo-physical properties. However, it is important to orient them in the direction of the expected load because in the direction perpendicular to the fibre orientation, the properties of the composite are much lower [6–10]. Combining the carbon fibres with magnesium, one of the lightest construction materials, with a density of  $1.8 \text{ g cm}^{-3}$ , can be obtained. These MMCs can meet the most severe weight-saving criteria and are of paramount interest in space-related activities. There is little knowledge about Mg composites reinforced with ultra-high modulus (UHM) carbon fibres in literature sources. The authors in [11], for instance, analysed the mechanical properties of an Mg-2 wt.% Li matrix reinforced with unidirectionally oriented T300 polyacrylonitrile

\*Corresponding author: tel.: +421 2 32401025; e-mail address: [juraj.korab@savba.sk](mailto:juraj.korab@savba.sk)



Fig. 1. The 3D component made of the Mg-C<sub>f</sub> composite.

(PAN) fibres and Granoc pitch-based carbon fibres (~ 45 vol.%). The effect of the interaction of fibres with the matrix on the microstructure and mechanical properties has been studied here.

Also, not many authors would venture into producing and testing 3D parts that may carry mechanical and thermal loads. Therefore, the main objective of this work was to design and produce a 3D-shape sample (strut joint) made of the Mg matrix reinforced with UHM continuous carbon fibres and test its mechanical and damping properties. Characterised and compared were two types of samples – those reinforced with carbon fibres and non-reinforced ones. The ultralight structural material might find various space-related applications, i.e., trusses, masts, frameworks for launchers, platforms and planetary habitats, solar arrays, attachment systems, kinematics mounts and fasteners, components for robots, rovers, etc. [12, 13].

## 2. Materials and methods

### 2.1. Materials used

The design of the 3-dimensional structural part is presented in Fig. 1. Dimensions of the component are as follows: the diameter of the base plate and the stem was 76 mm and 11 mm, respectively, and the overall height of the strut was 100 mm.

To produce the carbon fibre preform, several types of carbon fibres were used (Figs. 2–5). Continuous Granoc XN-90 pitch-type carbon fibres (Nippon Graphite Fiber Corporation) were used for unidirectional reinforcement of a stem/rod. The fibres have a



Fig. 2. Shaping in the Teflon tool of both the unidirectional reinforcement made of Granoc fibres and the PAN-type C-fibre fabric.



Fig. 3. The unidirectional reinforcement made of Granoc fibres bound with polyvinyl alcohol.

high modulus of elasticity (860 GPa) and low density ( $2.19 \text{ g cm}^{-3}$ ). During the preform production, continuous C-fibre bundles were immersed in a 5 wt.% aqueous solution of polyvinyl alcohol and inserted into a Teflon tool. Approximately 80 carbon fibre bundles, each with 6000 fibres, were used. Together with the mould, they were partially dried and subsequently pre-shaped to the form of the desired product that had a circular shape at one side (Fig. 3). Subsequently, the preform made of Granoc fibres was thoroughly dried and reinforced with a PAN-type C fabric at the circular end (Fig. 2). A complex shape preform with a

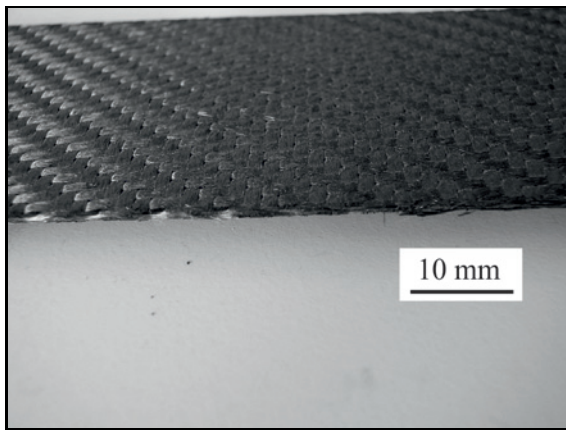


Fig. 4. Detail of a carbon fibre composite sheet.

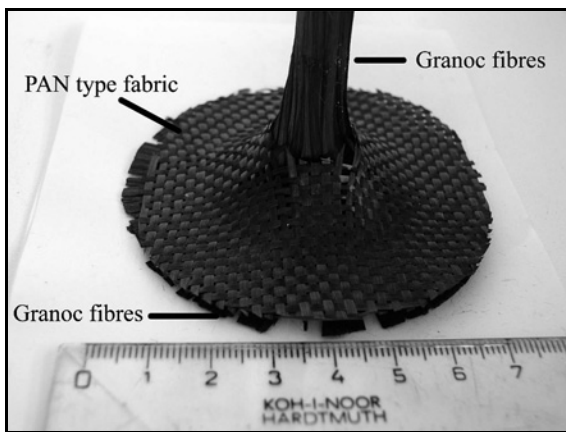


Fig. 5. Shaped fibre preform: Granoc C-fibre bundles spread to the circular shape. The PAN-type fabric is above.

weight of 17.1 g was placed into a carbon mould as a single piece. Finally, the carbon fibre composite sheet

(CeraMaterials, CC-16, density  $1.44 \text{ g cm}^{-3}$ ) of 1 mm thickness and 76 mm in diameter was attached to the circular part of the preform (Fig. 4). The finished preform was infiltrated with pure Mg, whereby the polymeric binder decomposed during heating to the infiltration temperature.

### 2.2. Technology

The Gas-assisted Pressure Infiltration (GPI) technology was used to produce two samples of the carbon-fibre reinforced component. In the beginning, a porous preform from continuous carbon fibres was inserted into a carbon die. Next, both the die and raw Mg were closed in a vacuum/pressure furnace and heated under low pressure of Ar protective gas to melting temperature. Once the Mg was melted and overheated to  $800^\circ\text{C}$ , the Ar gas was injected into a furnace under the pressure of 5–6 MPa and forced the liquid metal to fill the carbon fibre preform. Heating and melting were recorded by a data acquisition system and could be observed on a screen. A schematic of individual technological steps is presented in Fig. 6.

One non-reinforced sample was produced by the metal casting method, whereas the same carbon die was used. The weight of both types of 3D components was at a similar level ( $\sim 65 \text{ g}$ ).

### 2.3. Microstructural characterisation

After the bending test, the stem of the reinforced sample was cut in the direction normal to fibre orientation, and samples for metallographic examinations were prepared. A closer view of carbon fibre distribution in the Mg matrix was obtained by scanning electron microscopy (SEM) with a JEOL JSM 6610 microscope. The image analysis of different areas of the stem cross-section was performed by the Image J software.

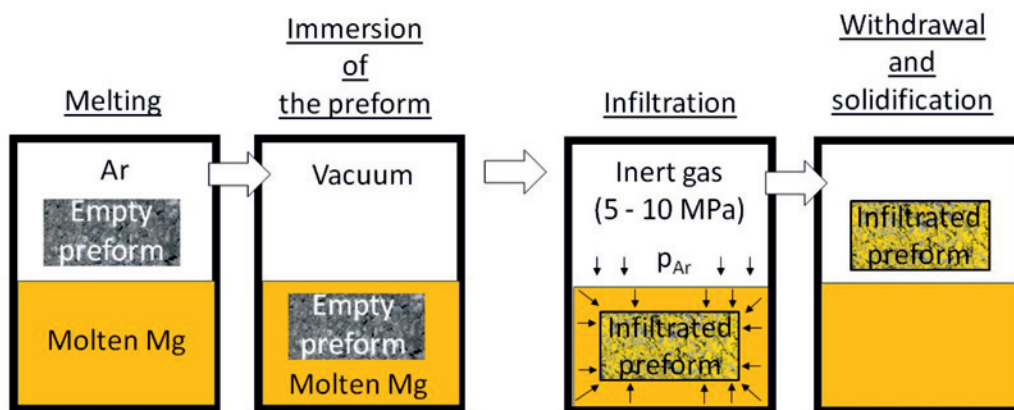


Fig. 6. The Gas Pressure Infiltration technology: description of individual steps.

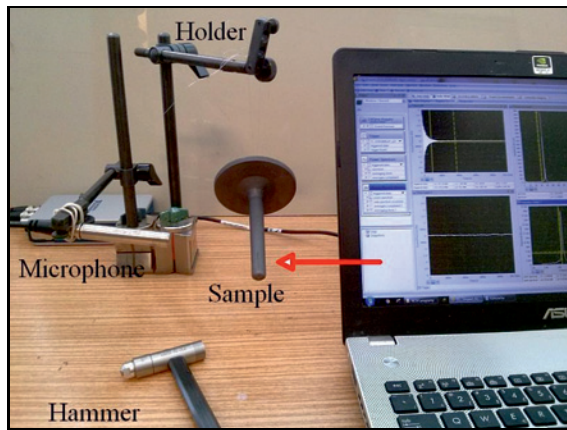


Fig. 7. The arrangement of the vibroacoustic test: measurement of eigenfrequencies. The component was excited with a hammer in the direction indicated by the red arrow.

Non-destructive examination of the whole infiltrated 3D-shape sample was performed by an X-ray tomography device (Nikon XT130V).

#### 2.4. Vibroacoustic testing

The 3D sample was hanged on a nylon thread during the vibroacoustic testing. The acoustic pressure was measured by a non-contact method, and the microphone instead of the accelerometer was used. This method was used because it was found that accelerometers were influencing the sample vibration very strongly. That is why the vibration of samples was actuated by a little hammer. The arrangement of the test is presented in Fig. 7.

#### 2.5. Bending tests

Bending tests were performed in a specially designed testing rig shown in Fig. 8. The circular part of the 3D-shape sample was fixed to a frame using a circular steel plate with an opening. The stem tip was inserted into a hole made in a special fixture at a distance of 5 mm from the stem end. This means that the tested length was not 100 mm (of the whole sample) but 95 mm. In the figure, the lower end of the special fixture is connected to a load cell and the upper one to a displacement transducer (W10 of HBM Company, Germany). The load cell was attached to a hydraulic piston (placed under the working table) that acted upwards and bent the sample in the same way via the fixture at a constant speed of  $1 \text{ mm min}^{-1}$ .

The stiffness ( $E$ ) was calculated for a rod loaded in a cantilever mode according to Eq. (1):

$$E = \frac{Fl^3}{3yJ}, \quad (1)$$

where  $F$  is the loading force acting at the end of the

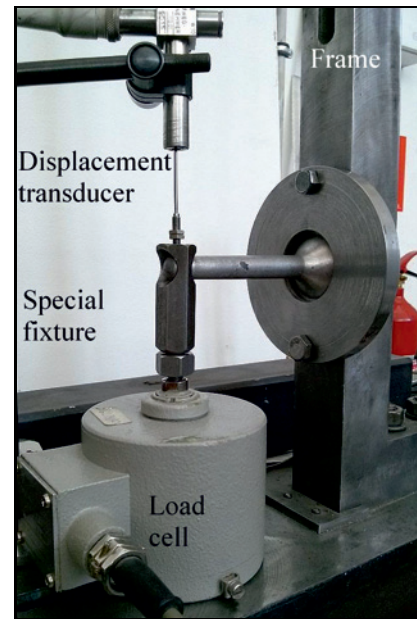


Fig. 8. A specially designed testing rig used for the bending test in a cantilever mode.

stem,  $L$  is the test span length,  $y$  is deflection, and  $J$  represents the moment of inertia for the stem that can be expressed by Eq. (2), where  $d$  represents the stem diameter:

$$J = \frac{\pi d^4}{64} \sim 0.05d^4. \quad (2)$$

### 3. Results and discussion

#### 3.1. Microstructure

A typical carbon fibre distribution in one cross-section of the stem is presented in Fig. 9. No pores were observed in the matrix and in the space between fibres that were squeezed together. Observed were regions where fibres are squeezed together and others where fibres show low volume fraction. However, the image analysis showed 40–45 vol.% of carbon fibres in the stem of the 3D component.

The X-ray photography did not reveal any pores inside the composite material (Figs. 10–12). The X-ray analysis confirmed the results obtained from metallographic observations, and both indicated a good quality of infiltration.

The weight of the demonstrator after infiltration was 65.54 g, its volume measured by the Archimedes method was  $36.5 \text{ cm}^3$ , and the calculated density of the whole reinforced 3D sample was  $1.796 \text{ g cm}^{-3}$ . The theoretical density obtained from material data of the composite material was  $1.84 \text{ g cm}^{-3}$ . From the weight of the carbon fibre preform (17.1 g), one can calculate

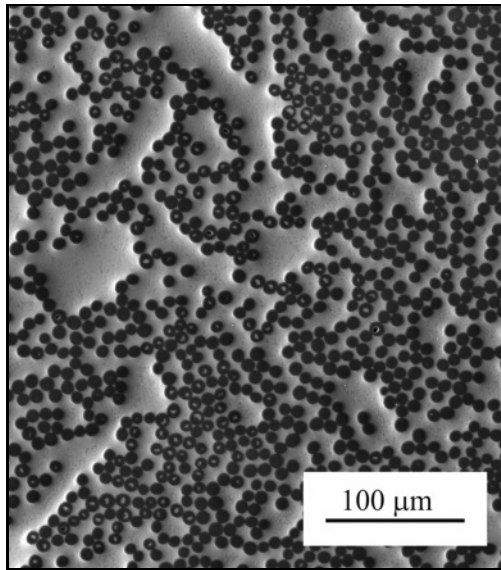


Fig. 9. The microstructure of the Mg-C<sub>f</sub> MMC. Distribution of carbon fibres in the stem of the 3D-shape component.

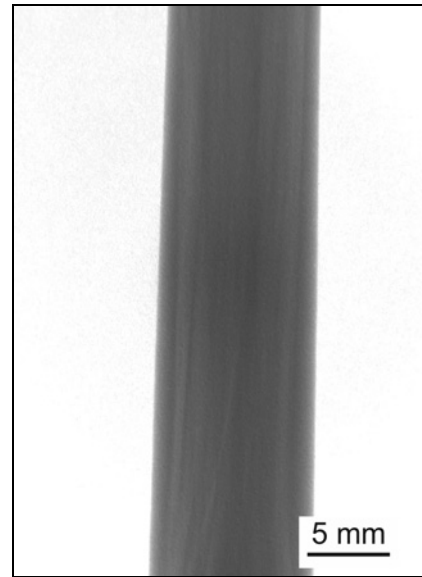


Fig. 11. X-ray photograph of the middle part of the stem.

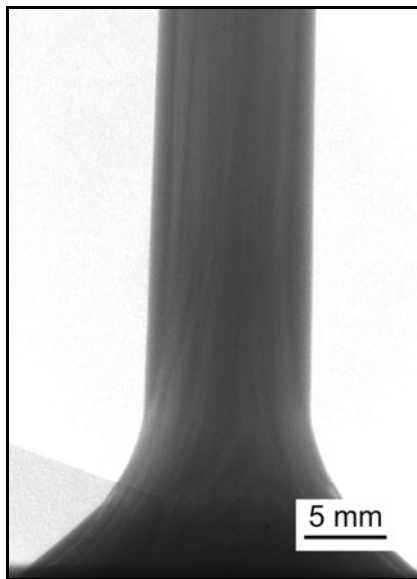


Fig. 10. X-ray photograph of the lower part of the 3D-shape component.

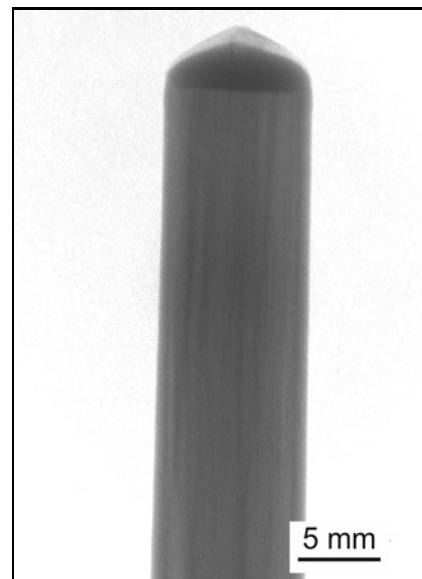


Fig. 12. X-ray photograph of the upper part of the stem.

the overall volume fraction of the reinforcement at the level of 26 vol. %.

### 3.2. Vibroacoustic testing

Vibroacoustic tests served for the non-destructive characterisation of two materials – the reinforced and non-reinforced. The loss factor was calculated accord-

ing to Eq. (3):

$$\eta = \frac{dF}{F_0}, \quad (3)$$

where values of  $dF$  and  $F_0$  are frequencies obtained from charts, frequency vs. sound pressure level (Figs. 13, 14). The calculated loss factor for two composite material samples was  $\eta_{mmc1} = 0.0018$  and  $\eta_{mmc2} = 0.0021$ , and for the sample made of pure Mg, a value  $\eta_{Mg} = 0.0008$  was obtained. The measurements confirmed that samples reinforced with carbon

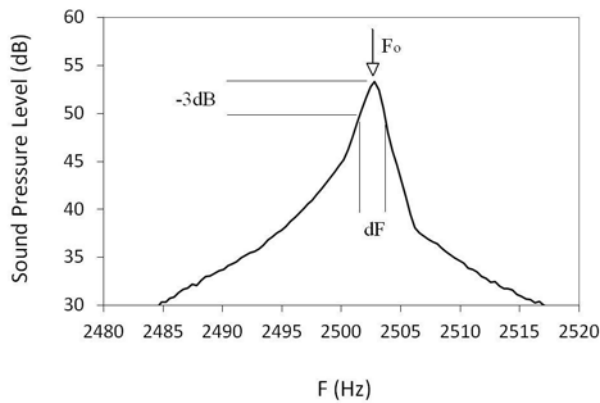


Fig. 13. The record used to calculate the loss factor for the sample made of pure Mg.

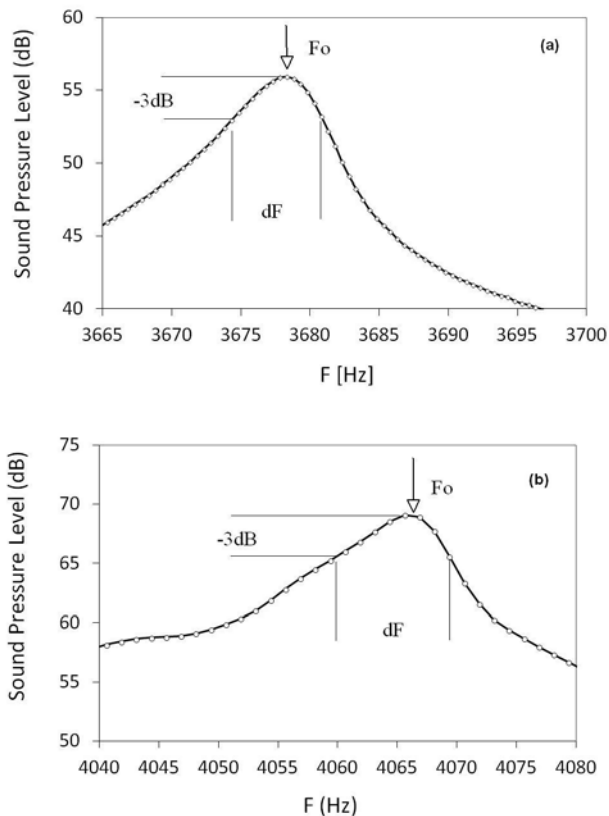


Fig. 14. Recordings used to calculate the loss factor for samples made of the Mg-C<sub>f</sub> composite: (a) sample No. 1 and (b) sample No. 2.

fibres had approximately two times better damping than those made of pure Mg.

The measurement presented in Fig. 15 shows that samples of the Mg-C<sub>f</sub> composite material had higher eigenfrequencies (black and red line), which indicated higher stiffness compared to the unreinforced sample

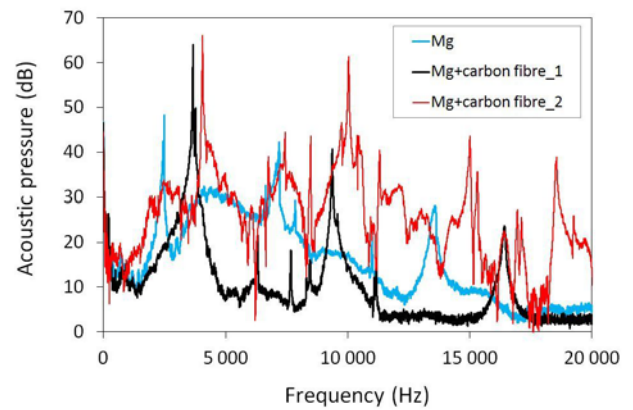


Fig. 15. Eigenfrequencies of individual samples: one sample made of pure Mg and two samples made of the Mg-C<sub>f</sub> composite.

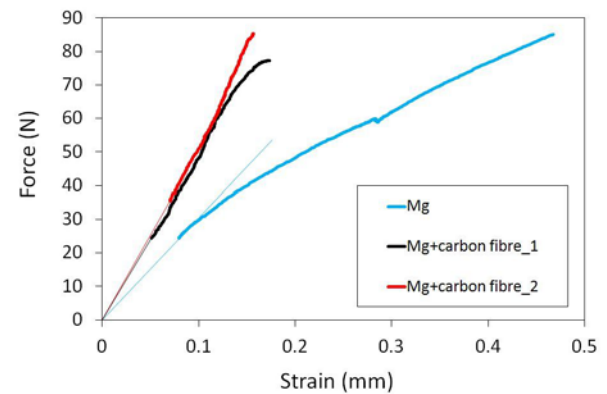


Fig. 16. Recordings of the early stage of the bending test: the sample made of pure magnesium (blue line) and the Mg-C<sub>f</sub> composite material (black and red lines).

(blue line). In the figure, a difference between the vibrational spectra of both Mg-C<sub>f</sub> composites can be observed. We explain this phenomenon as the result of a non-uniform and different distribution of carbon fibres in the Mg-matrix in both composites.

Both types of non-destructive testing indicated that the 3D-shape sample made of the Mg-C<sub>f</sub> composite presented higher stiffness than the part made of pure Mg.

### 3.3. Mechanical properties

Mechanical tests were used to detect differences in the behaviour of two different materials. Due to technical and handling difficulties with a special fixture, a specific preload to the sample was always present. That is why recordings started at the load of 25 N. The detail of the beginning of the test is shown in Fig. 16, and the whole recording is seen in Fig. 17, where the scale of the measurement can be seen.

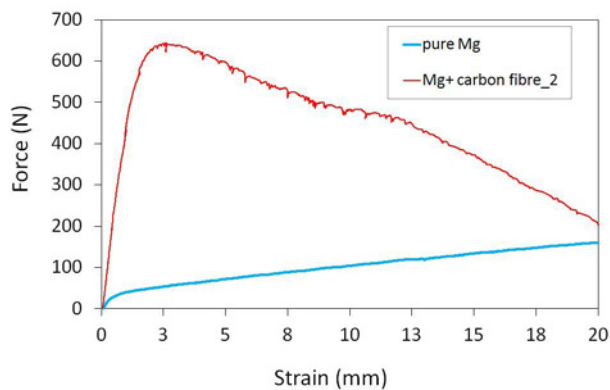


Fig. 17. Bending test – the whole test record.

The stiffness was calculated according to Eqs. (1) and (2). The calculation was performed for a simplified case when a rod was fixed in the cantilever mode and loaded with force at the end of the rod. It was because the main aim of the paper was not to focus on the calculation of the exact values of the modulus of elasticity but to compare the mechanical behaviour of these two different materials – reinforced and non-reinforced. That is why the authors neglected the boundary conditions at the clamping side of the 3D component.

Results showed that the  $E$ -modulus of the reinforced sample was much higher (185 GPa) than that of the unreinforced Mg material (28 GPa). Similar results (180 GPa) were obtained in [11], where the same type of material was characterised (Mg matrix was reinforced with the continuous Pitch-type Granoc fibres). Here, rectangular samples with dimensions  $50 \times 10 \times 3 \text{ mm}^3$  were cut out from the bulk composite and were examined in the longitudinal direction. The comparison made for tested, theoretical (the rule of mixtures, ROM), and other experimental data [11] showed that both experimental data are similar and are far lower than theoretical calculations. Experimental results confirmed that the strengthening potential of Granoc fibres was probably not fully reached. Theoretical calculations according to the ROM show that the  $E$ -modulus for the stem (a bar with a diameter of 11 mm and length of 100 mm) reinforced with 40 vol.% of fibres should be at the level of 368 GPa. Obtained experimental values were probably lower due to both the poorly reinforced conical part of the component and the non-homogeneous distribution of fibre bundles squeezed to the centre of the stem.

#### 4. Conclusions

The mechanical and vibroacoustic properties of the 3D sample made of pure Mg or the Mg-C<sub>f</sub> compos-

ite were characterised. In the composite, the metal matrix was reinforced with continuous carbon fibres. The work aimed to demonstrate that such structural components could be produced by the gas pressure infiltration technology and to characterise some chosen mechanical properties.

From obtained data, it can be concluded that in comparison to the non-reinforced material, the carbon fibre reinforced 3D sample showed:

- about six times higher  $E$ -modulus (185 GPa vs. 28 GPa),
- similar weight  $\sim 65 \text{ g}$ .

Microstructural analysis and results of measurements confirmed that the Mg-C<sub>f</sub> composite is suitable for producing structural parts for different space applications, i.e., trusses, masts frameworks for launchers, platforms and planetary habitats, fasteners, components for robots. It was also demonstrated that non-porous composite material could be produced by gas pressure infiltration technology.

#### Acknowledgements

This research was funded by the European Space Agency, Contract No: 4000117031/16/NL/NDe, under the name: “Novel magnesium composites for ultralight structural components,” the project “Building-up Centre for Advanced Materials Application” of the Slovak Academy of Sciences, ITMS project code 313021T081 supported by Research & Innovation Operational Programme funded by the ERDF, and by the Slovak Grant Agency (VEGA grant No. 2/0117/20).

#### Special acknowledgement

The authors would like to thank their colleague *Peter Tobolka*, who performed the mechanical and vibroacoustic measurements used in this paper.

#### References

- [1] J. Ajaja, F. Barthelat, Damage accumulation in a carbon fiber fabric reinforced cyanate ester composite subjected to mechanical loading and thermal cycling, *Compos. Part B: Engineering* 90 (2016) 523–529. <https://doi.org/10.1016/j.compositesb.2015.09.054>
- [2] S. P. Rawal, Metal-matrix composites for space applications, *J. Met.* 53 (2001) 14–17. <https://doi.org/10.1007/s11837-001-0139-z>
- [3] M. M. Ali, N. Nived, Composites materials for sustainable space industry: A review of recent developments, *World Rev. Sci. Technol.* 17 (2021) 172–196. <https://dx.doi.org/10.1504/WRSTSD.2021.114680>

- [4] M. May, G. D. Rupakula, P. Matura, Non-polymer-matrix composite materials for space applications, *Compos. Part C: Open Acces.* 3 (2020) 100057.  
<https://doi.org/10.1016/j.jcomc.2020.100057>
- [5] G. De Zanet, A. Viquerat, Thermal response of CFRP deployable tubes in the space environment, *AIAA Scit. Tech. 2020 Forum.*  
<https://doi.org/10.2514/6.2020-1439>
- [6] M. Russell-Stevens, R. Todd, M. Papakyriacou, Microstructural analysis of a carbon fibre reinforced AZ91D magnesium alloy composite, *Surf. Interface Anal.* 37 (2005) 336–342.  
<https://doi.org/10.1002/sia.2026>
- [7] M. K. Hassanzadeh-Aghdam, R. Ansari, Role of fiber arrangement in the thermal expanding behavior of unidirectional metal matrix composites, *Mater. Chem. Phys.* 252 (2020) 123273.  
<https://doi.org/10.1016/j.matchemphys.2020.123273>
- [8] D. M. Goddard, P. D. Burke, D. E. Kizer, Continuous Graphite Fiber MMC's in Engineered Materials, *Handbook 1 (1987), Vol. 1 Composites.* Edited by C. A. Dostal et al. ASM International, Metals Park, 1987.
- [9] K. U. Kainer, *Custom-made Materials for Automotive and Aerospace Engineering*, John Wiley & Sons, New York, 2006. ISBN: 978-3-527-31360-0
- [10] A. B. Spierings, K. Dawson, T. Heeling, P. J. Uggowitzer, R. Schäublin, F. Palm, K. Wegener, Microstructural features of Sc- and Zr-modified Al-Mg alloys processed by selective laser melting, *Mater. Des.* 115 (2017) 52–63.  
<https://doi.org/10.1016/j.matdes.2016.11.040>
- [11] S. Kúdela Jr., O. Bajana, L. Orovčík, P. Rachanowski, P. Z. Rachanowski, Strengthening in MgLi matrix composites reinforced with unidirectional T300 and Granoc carbon fibres, *Kovove Mater.* 58 (2020) 223–231.  
<https://doi.org/10.4149/km.2020.4.223>
- [12] R. J. Rioja, The evolution of Al-Li base products for aerospace and space applications, *Metall. Mater. Trans. A* 43 (2012) 3325–3337.  
<https://doi.org/10.1007/s11661-012-1155-z>
- [13] A. J. Juhasz, G. P. Peterson, Review of advanced radiator technologies for spacecraft power systems and space thermal control, *NASA Technical Memorandum*, 4555, TP-4555, 1994.
- [14] Z. S. Zoor, Space applications of composite materials, *J. Space Technol.* 8 (2018) 65–70.